

Pressure-induced superconductivity in $\text{Eu}_{0.5}\text{Ca}_{0.5}\text{Fe}_2\text{As}_2$: FeAs-based superconductivity hidden by antiferromagnetism of Eu sublattice

Akihiro Mitsuda,* Tomohiro Matoba, and Hirofumi Wada

Department of Physics, Kyushu University, 6-10-1 Hakozaki, Higashi-ku, Fukuoka 812-8581, Japan

Fumihiko Ishikawa

Graduate School of Science and Technology, Niigata University, Niigata 950-2181, Japan

Yuh Yamada

Department of Physics, Niigata University, Niigata 950-2181, Japan

(Dated: January 10, 2022)

To clarify superconductivity in EuFe_2As_2 hidden by antiferromagnetism of Eu^{2+} , we investigated a Ca-substituted sample, $\text{Eu}_{0.5}\text{Ca}_{0.5}\text{Fe}_2\text{As}_2$, under high pressure. For ambient pressure, the sample exhibits a spin-density-wave (SDW) transition at $T_{\text{SDW}} = 191$ K and antiferromagnetic order at $T_{\text{N}} = 4$ K, but no evidence of superconductivity down to 2 K. The Ca-substitution certainly weakens the antiferromagnetism. With increasing pressure, T_{SDW} shifts to lower temperature and becomes more unclear. Above 1.27 GPa, pressure-induced superconductivity with zero resistivity is observed at around $T_{\text{c}} = 20$ K. At 2.14 GPa, T_{c} reaches a maximum value of 24 K and the superconducting transition becomes the sharpest. These features of emergence of the superconductivity are qualitatively similar to those observed in AFe_2As_2 ($\text{A} = \text{Ba}, \text{Ca}$).

PACS numbers: 74.62.Fj, 74.62.Dh, 74.25.Dw, 74.70.Dd

Since Kamihara et al. found that $\text{LaFeAsO}_{1-x}\text{F}_x$ for $0.05 \leq x \leq 0.12$ is a high- T_{c} superconductor of $T_{\text{c}} = 26$ K,¹ a lot of active researches on Fe-based superconductors have been started all over the world. Presently, replacing La with other lanthanides raised T_{c} up to 55 K, which is the highest T_{c} value except the high- T_{c} cuprates.² The parent material LaFeAsO crystallizes in the tetragonal ZrCuSiAs type structure, in which LaO and FeAs layers are stacked alternately, and performs a structural phase transition from tetragonal to orthorhombic symmetry at 155 K^{3,4} and a spin-density-wave (SDW) transition at 137 K.³ Either F-doping or oxygen vacancies, which corresponds to electron doping, suppresses these transitions and induces superconductivity.¹ Though Fe is a magnetic element, which has been considered as destructive to superconductivity, it is intriguing that the FeAs layer plays a key role to giving rise to the superconductivity.

Through the active researches, similar superconductivity of $T_{\text{c}} = 38$ K was found also in $\text{Ba}_{1-x}\text{K}_x\text{Fe}_2\text{As}_2$.⁵ This system forms the tetragonal ThCr_2Si_2 type structure, which consists of alternate stacking of a Ba/K layer and similar FeAs layer to that in LaFeAsO . Similarly to LaFeAsO , the parent compound BaFe_2As_2 exhibits the SDW transition at 140 K.^{5,6} Substitution of K for Ba, which corresponds to hole doping, induces the superconductivity, accompanied by collapse of the SDW transition.⁵ In addition, applying external pressure⁷ and/or chemical pressure^{8,9} (isovalent substitution of P for As) also induces the superconductivity. EuFe_2As_2 with the same structure as BaFe_2As_2 exhibits the SDW transition due to Fe at 190 K and antiferromagnetic order of Eu^{2+} at 20 K.¹⁰ With increasing pressure, the SDW transition is continuously collapsed and a sharp

drop at 30 K in electrical resistivity appears at around 2 GPa, which is reminiscent of superconductivity. After the drop, however, the resistivity goes to a finite value (not zero resistivity) at around 20 K, where the antiferromagnetic order occurs.¹¹ It is speculated that cooper pairs should be destroyed by molecular field due to antiferromagnetism (AFM) of Eu^{2+} ions as is observed in HoMo_6S_8 ¹² and $\text{HoNi}_2\text{B}_2\text{C}$.¹³ To clarify the superconducting properties hidden by the antiferromagnetic order of Eu^{2+} , we try to weaken the molecular field by 50% diluting Eu^{2+} by nonmagnetic isovalent Ca^{2+} , which corresponds to decrease in number of magnetic moments of Eu^{2+} without carrier doping. Additionally, the diluted sample was investigated under high pressure. In the present study, we report pressure-induced superconductivity and zero resistivity in $\text{Eu}_{0.5}\text{Ca}_{0.5}\text{Fe}_2\text{As}_2$. It is shown that Eu ions enhance superconducting transition temperature T_{c} .

The single crystal of $\text{Eu}_{0.5}\text{Ca}_{0.5}\text{Fe}_2\text{As}_2$ was grown in a tin flux. A mixture of constituent elements in the ratio of $\text{Eu} : \text{Ca} : \text{Fe} : \text{As} : \text{Sn} = 0.5 : 0.5 : 2 : 2 : 48$, which was put into an alumina crucible, was heated at 1000°C for 24 hours in a quartz tube, where 1/3-atm Ar gas at room temperature was sealed. Subsequently, the mixture was cooled down to 500°C at the rate of $-14^\circ\text{C}/\text{h}$ and the tin flux was removed by a centrifuge. We obtained many pieces of plate-like single crystals with typical dimensions of $\sim 3 \times 3 \times 0.1$ mm³. Powder x-ray diffraction pattern at room temperature exhibits a single phase which crystallizes in the tetragonal ThCr_2Si_2 type structure with lattice constants of $a = 3.897$ Å and $c = 12.006$ Å. These values lie almost halfway between EuFe_2As_2 ($a = 3.902$ Å and $c = 12.138$ Å) and CaFe_2As_2 ($a = 3.886$ Å and $c = 11.776$ Å), which are also synthe-

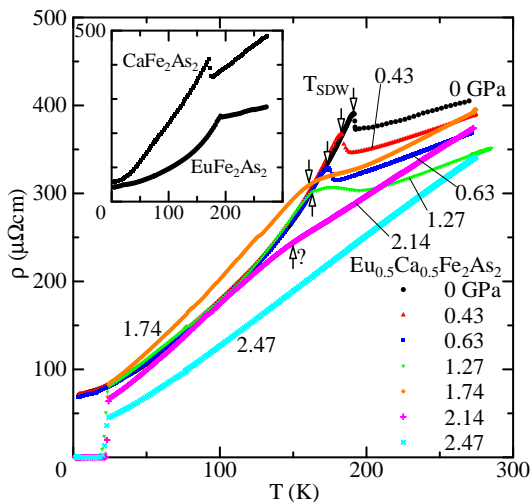


FIG. 1: Electrical resistivity versus temperature of $\text{Eu}_{0.5}\text{Ca}_{0.5}\text{Fe}_2\text{As}_2$ at various pressures. The open arrows depict spin-density-wave (SDW) temperature, T_{SDW} . However, T_{SDW} is difficult to determine at 2.14 GPa. The inset exhibits temperature dependence of the resistivity of CaFe_2As_2 and EuFe_2As_2 synthesized by our group.

sized by our group. The lattice constants of both end compounds are in good agreement with those reported in Ref. 10,14. The Energy dispersive X-ray (EDX) spectroscopy confirms that composition of the sample is almost $\text{Eu} : \text{Ca} : \text{Fe} : \text{As} = 0.5 : 0.5 : 2 : 2$. These results suggest 50% Eu atoms are substituted by Ca atoms homogeneously. Electrical resistivity under high pressure was measured with current flowing in the ab plane by using an ac resistance bridge (LR-700, Linear Research) in the temperature range between 4.2 and 280 K. Pressure was generated up to 2.47 GPa by using a piston-cylinder type pressure cell, which consists of inner (NiCrAl alloy) and outer (CuBe alloy) cylinders. The sample and a tin manometer were placed into a Teflon cell filled with a pressure transmitting medium of mixture of 2 types of Fluorinert in the ratio of FC70 : FC77 = 1 : 1. The Teflon cell was inserted into the pressure cell and pressed by pistons made of nonmagnetic tungsten carbide. Magnetization measurement under high pressure was carried out by a SQUID magnetometer (MPMS, Quantum Design) in the temperature range between 2 and 300 K. Pressure was generated up to 0.8 GPa by basically the same method as in the resistivity measurement. We used a pressure cell made of nonmagnetic CuTi alloy and pistons made of zirconia to reduce a magnetization signal from the pressure cell. Many pieces of small single crystals directed randomly were used in the magnetization measurement. To obtain magnetization of the sample, magnetization of the pressure cell was subtracted from the measured value.

Figure 1 demonstrates temperature dependence of electrical resistivity ρ of $\text{Eu}_{0.5}\text{Ca}_{0.5}\text{Fe}_2\text{As}_2$ under various pressures. In addition, the ρ - T curves of CaFe_2As_2 and

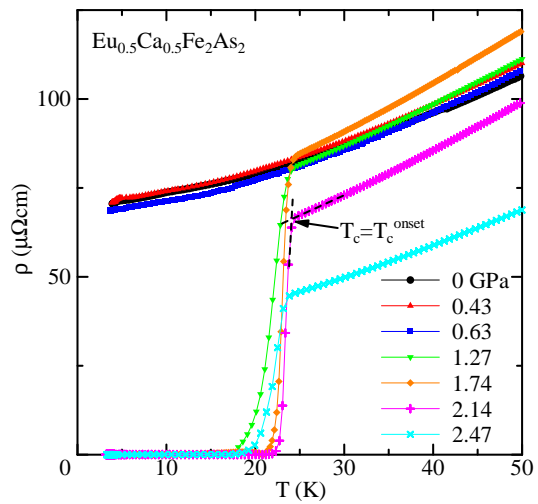


FIG. 2: Electrical resistivity versus temperature of $\text{Eu}_{0.5}\text{Ca}_{0.5}\text{Fe}_2\text{As}_2$ at various pressures in the low temperature region. The short dash line depicts how to define onset superconducting temperature T_c^{onset} .

EuFe_2As_2 synthesized by our group, of which T_{SDW} are 170 K and 191 K, respectively, are also shown in the inset. These curves qualitatively coincide with those reported in Ref. 10,14,15. The behavior of $\text{Eu}_{0.5}\text{Ca}_{0.5}\text{Fe}_2\text{As}_2$ for ambient pressure is intermediate between both end compounds. A sharp cusp, which corresponds to spin-density-wave (SDW) transition, is observed at $T_{\text{SDW}} = 191$ K. T_{SDW} is closed to that of EuFe_2As_2 ,¹⁰ but shape of the cusp is similar to that of CaFe_2As_2 .¹⁵ Below T_{SDW} , with decreasing temperature, the resistivity decreases significantly with concave-up curvature down to $70 \mu\Omega\text{cm}$ without any anomalies like superconductivity or AFM of Eu^{2+} . Unlike $\text{Eu}_{0.5}\text{K}_{0.5}\text{Fe}_2\text{As}_2$,¹⁶ substitution of iso-valent Ca for Eu neither collapses the SDW transition nor induces superconductivity. At 0.43 and 0.63 GPa, except for T_{SDW} , which shifts to lower temperatures with increasing pressure, temperature dependence of ρ is qualitatively the same as that at ambient pressure. At 1.27 GPa, superconductivity suddenly appears at around 23 K, which is much higher than that of CaFe_2As_2 . The cusp of the SDW transition transforms into a broad maximum. The ρ - T curve is comparably similar to that below 0.63 GPa except for the superconducting behavior and the shape of T_{SDW} , which exhibits this pressure is critical pressure P_c . At 1.74 GPa, complete zero resistivity is realized and the superconducting transition becomes sharper than that at 1.27 GPa, which suggests more homogeneous superconductivity. The anomaly associated with the SDW transition becomes broader and more indistinct. The slope of the ρ - T curve above T_{SDW} becomes larger. These features result in considerable change of the shape of the ρ - T curve. At 2.14 GPa, the sharp superconducting transition shifts to a little higher temperature, which demonstrates maximum T_c of 24 K in the present study. The anomaly of the SDW transition can be seen

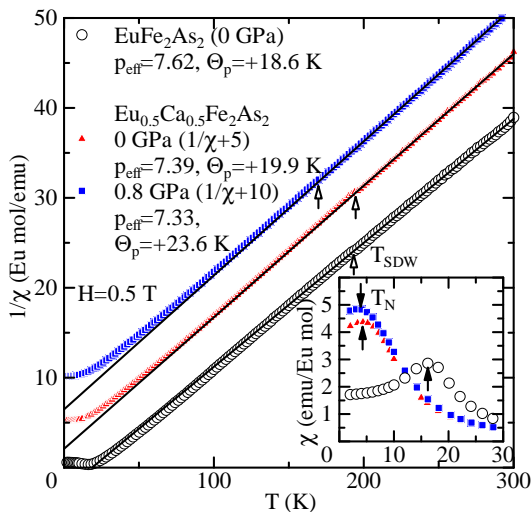


FIG. 3: Inverse susceptibility versus temperature of EuFe_2As_2 at 0 GPa and of $\text{Eu}_{0.5}\text{Ca}_{0.5}\text{Fe}_2\text{As}_2$ at 0 and 0.8 GPa. The open arrows depict spin-density-wave (SDW) temperature. The solid lines exhibits Curie-Weiss law. The inset demonstrates temperature dependence of magnetic susceptibility in the low temperature region. The solid arrows show the Néel temperature.

as slight convex-up behavior at around 150 K, but is too shallow to determine T_{SDW} precisely. The residual resistivity ρ_0 , which is determined as the ρ value just above T_c , begins to drop. Finally, at 2.47 GPa, again the transition becomes less sharp and shift to lower temperature, which is possibly onset of collapse of the superconductivity as is observed in CaFe_2As_2 ^{17,18} and BaFe_2As_2 .⁷ The ρ - T curve above T_c exhibits concave up behavior and no anomaly, which indicates the SDW transition is collapsed completely. The ρ_0 value decreases down to $\sim 45 \mu\Omega\text{cm}$. Similar drop of ρ_0 with pressure is observed also in CaFe_2As_2 .^{17,18}

Figure 3 shows temperature dependence of inverse magnetic susceptibility $1/\chi$ of EuFe_2As_2 at 0 GPa and of $\text{Eu}_{0.5}\text{Ca}_{0.5}\text{Fe}_2\text{As}_2$ at 0 and 0.8 GPa. The inset indicates the χ - T curves in the low temperature region. For EuFe_2As_2 , the data is almost in accordance with the previous one.¹⁰ There exist a clear peak in the χ - T curve at $T_N = 17$ K and a kink in the $1/\chi$ - T curve at $T_{\text{SDW}} = 193$ K. Above T_{SDW} , the susceptibility obeys the Curie-Weiss (CW) law with an effective moment p_{eff} of $7.62\mu_B/\text{Eu}$ and a Weiss temperature Θ_p of $+18.6$ K. The p_{eff} value is close to the theoretical value ($7.94\mu_B/\text{Eu}$) of a free Eu^{2+} ion. The positive Θ_p value suggests a ferromagnetic interaction. Actually, a comparably small magnetic field of ~ 1 T can saturate magnetization.¹⁰ Substituting Eu with Ca by 50 % lowers T_N down to 4 K, but nearly retains the CW behavior. The former means that the AFM is destabilized, which results from depression of RKKY (Ruderman-Kasuya-Kittel-Yosida) interaction due to dilution of magnetic Eu^{2+} ions. The latter implies that the Eu valence remains almost $2+$. With ap-

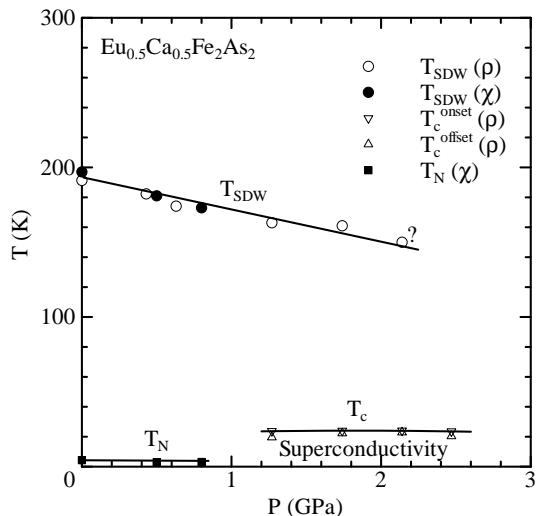


FIG. 4: Temperature versus pressure phase diagram of $\text{Eu}_{0.5}\text{Ca}_{0.5}\text{Fe}_2\text{As}_2$. The T_c^{onset} value has a faint maximum of 24 K at around 2.14 GPa.

plying pressure to $\text{Eu}_{0.5}\text{Ca}_{0.5}\text{Fe}_2\text{As}_2$, T_{SDW} is lowered, as shown also in Fig. 1, but the T_N value and the CW behavior, which are associated with Eu, are nearly unchanged. This means that the valence and the magnetism of Eu are insensitive to pressure. We also measured magnetization curves at 1.8 K. (not shown) At both 0 and 0.8 GPa, the magnetization is saturated to $6.5\mu_B/\text{Eu}$, which is close to magnetic moment of Eu^{2+} of $7\mu_B/\text{Eu}$. This also supports Eu valence remains close to $2+$ under pressures up to 0.8 GPa. We speculate that the magnetism and the valence of Eu are probably preserved also under higher pressures than 0.8 GPa. To investigate competition between the magnetism of Eu and the superconductivity in more detail, magnetization measurements under higher pressure are now in progress.

To summarize the present experiments, the T - P phase diagram is shown in Fig. 4. We define T_c^{offset} as temperature where the resistivity reaches 10% of the residual resistivity ρ_0 . As T_{SDW} is being suppressed with increasing pressure, the superconductivity of $T_c \sim 20$ K emerges suddenly at around 1.2 GPa. Pressure dependence of T_c is quite small but has a faint maximum of 24 K at around 2.14 GPa, where the superconducting transition is the sharpest. The AFM of Eu^{2+} is realized at around 4 K. Since T_N is much lower than T_c unlike EuFe_2As_2 , it seems that the superconductivity is realized stably in spite of the AFM.

Compared with CaFe_2As_2 ($P_c \sim 0.4$ GPa and $T_c \sim 10$ K),^{17,18} both P_c and T_c are quite higher in $\text{Eu}_{0.5}\text{Ca}_{0.5}\text{Fe}_2\text{As}_2$ ($P_c \sim 1.3$ GPa and $T_c \sim 24$ K), which indicates that the superconductivity observed in this study is not due to an impurity of CaFe_2As_2 but intrinsic. In addition, it is suggested that Eu ions play a key role in enhancing T_c . Though a structural phase transition from tetragonal to collapsed tetragonal type takes place above 0.8 GPa in CaFe_2As_2 , there exists no evi-

dence of such a structural transition under high pressures up to 2.47 GPa in $\text{Eu}_{0.5}\text{Ca}_{0.5}\text{Fe}_2\text{As}_2$. On the other hand, compared with EuFe_2As_2 ($P_c \sim 2.0$ GPa and $T_c \sim 30$ K, but no zero resistivity due to AFM of Eu^{2+}),¹¹ both P_c and T_c are lower in the present system. Since lattice volume of $\text{Eu}_{0.5}\text{Ca}_{0.5}\text{Fe}_2\text{As}_2$ is smaller by 1.4% than that of EuFe_2As_2 , it can be regarded that chemical pressure is applied in addition to hydrostatic pressure in the present study. As a result, P_c in $\text{Eu}_{0.5}\text{Ca}_{0.5}\text{Fe}_2\text{As}_2$ is smaller than that in EuFe_2As_2 (~ 2.0 GPa).¹¹ Eu ions has two opposite effects. One is to induce superconductivity of $T_c \sim 30$ K. The other is to destroy cooper pairs through the AFM. Dilution of Eu by Ca weakens both effects, which results in decrease in T_c and appearance of zero resistivity. Recently Terashima et al. have reported that EuFe_2As_2 becomes a superconductor with zero resistivity under high pressure of 2.8 GPa.¹⁹ Matsubayashi et al. also observe zero resistivity in EuFe_2As_2 in the quite narrow pressure range of 2.7 \sim 2.8 GPa.²⁰ In the limited pressure range of ~ 2.8 GPa, the superconductivity might slightly overcome the AFM. Very recently, Zheng et al. demonstrate that both diluting Eu with Sr or Ba and substitution of Co for Fe induces superconductivity with zero resistivity,²¹ which coincides with our results.

The chemical and hydrostatic pressures are also expected to induce valence transition from Eu^{2+} toward Eu^{3+} because Eu^{2+} has larger volume than Eu^{3+} does. However, the effective magnetic moment and the spontaneous magnetization remain the values for a Eu^{2+} ion under pressures up to 0.8 GPa in the present system. There exists no evidence of Eu valence change in the present study.

In conclusion, we observed pressure-induced superconductivity ($T_c \sim 24$ K) with zero resistivity of $\text{Eu}_{0.5}\text{Ca}_{0.5}\text{Fe}_2\text{As}_2$ in the pressure range of $P = 1.27 \sim 2.47$ GPa. Diluting Eu with isovalent Ca weakens the AFM of Eu^{2+} with preserving the SDW and the CW behavior. It is strongly suggested that in EuFe_2As_2 the AFM of Eu^{2+} and the pressure-induced superconductivity compete with each other. Substitution of Ca and/or applying pressure seem not to change Eu valence.

Acknowledgments

The authors thank Dr. M. Watanabe at Center of Advanced Instrumental Analysis, Kyushu University for helping us to perform SEM-EDX analysis.

* Electronic address: 3da@phys.kyushu-u.ac.jp

¹ Y. Kamihara, T. Watanabe, M. Hirano, and H. Hosono, *J. Am. Chem. Soc.* **130**, 3296 (2008).
² X. F. Chen, T. Wu, G. Wu, R. H. Liu, H. Chen, and D. F. Fang, *Nature (London)* **453**, 761 (2008).
³ C. de la Cruz, Q. Huang, J. W. Lynn, J. Li, W. Ratcliff II, H. A. Mook, G. F. Chen, J. L. Luo, N. L. Wang, and Pengcheng Dai, *Nature (London)* **453**, 899(2008).
⁴ T. Nomura, S.W. Kim, Y. Kamihara, M. Hirano, P. V. Sushko, K. Kato, M. Takata, A. L. Shluger, and H. Hosono, *Supercond. Sci. Technol.* **21**, 125028 (2008).
⁵ M. Rotter, M. Tegel, and D. Johrendt, *Phys. Rev. Lett.* **101**, 107006 (2008).
⁶ M. Rotter, M. Tegel, and D. Johrendt, *Phys. Rev. B* **78**, 020503 (2008).
⁷ F. Ishikawa, N. Eguchi, M. Kodama, K. Fujimaki, M. Einaga, A. Ohmura, A. Nakayama, A. Mitsuda, and Y. Yamada, *Phys. Rev. B* **79**, 172506 (2009).
⁸ S. Jiang, H. Xing, G. Xuan, C. Wang, Z. Ren, C. Feng, J. Dai, Z. Xu, and G. Cao, *J. Phys.: Condens. Matter* **21**, 382203 (2009).
⁹ S. Kasahara, T. Shibauchi, K. Hashimoto, K. Ikada, S. Tonegawa, H. Ikeda, H. Takeya, K. Hirata, T. Terashima, and Y. Matsuda, arXiv:0905.4427 (2009).
¹⁰ Z. Ren, Z. Zhu, S. Jiang, X. Xu, Q. Tao, C. Wang, C. Feng, G. Cao, and Z. Xu, *Phys. Rev. B* **78**, 052501 (2008).
¹¹ C. F. Miclea, M. Nicklas, H. S. Jeevan, D. Kasinathan, Z. Hossain, H. Rosner, P. Gegenwart, C. Geibel, and F.

Steglich, *Phys. Rev. B* **79**, 212509 (2009).
¹² M. Ishikawa and Ø. Fischer, *Solid State Commun.* **23**, 37 (1977).
¹³ H. Eisaki, H. Takagi, R. J. Cava, B. Batlogg, J. J. Krajewski, W. F. Peck, Jr., K. Mizuhashi, J. O. Lee, and S. Uchida, *Phys. Rev. B* **50**, 647 (1994).
¹⁴ T. Park, E. Park, H. Lee, T. Klimczuk, E. D. Bauer, F. Ronning, and J. D. Thompson, *J. Phys. condens. Matter* **20** 322204 (2008).
¹⁵ N. Ni, S. Nandi, A. Kreyssig, A. I. Goldman, E. D. Mun, S. L. Bud'ko, and P. C. Canfield, *Phys. Rev. B* **78**, 014523 (2008).
¹⁶ H. S. Jeevan, Z. Hossain, Deepa Kasinathan, H. Rosner, C. Geibel, and P. Gegenwart, *Phys. Rev. B* **78** 092406 (2008).
¹⁷ M. S. Torikachvili, S. L. Bud'ko, N. Ni, and P. C. Canfield, *Phys. Rev. Lett.* **101**, 057006 (2008).
¹⁸ H. Lee, E. Park, T. Park, V. A. Sidorov, F. Ronning, E. D. Bauer, and J. D. Thompson, *Phys. Rev. B* **80**, 024519 (2009).
¹⁹ T. Terashima, M. Kimata, H. Satsukawa, A. Harada, K. Hazama, S. Uji, H. S. Suzuki, T. Matsumoto, and K. Murata, *J. Phys. Soc. Jpn.* **78**, 083701 (2009).
²⁰ K. Matsubayashi, in preparation
²¹ Q. J. Zheng, Y. He, T. Wu, G. Wu, H. Chen, J. J. Ying, R. H. Liu, X. F. Wang, Y. L. Xie, Y. J. Yan, Q. J. Li, and X. H. Chen, arXiv:0907.5547v1.